CrossMark

ORIGINAL PAPER

Mechanisms of large deformation in soft rock tunnels: a case study of Huangjiazhai Tunnel

Kang Bian[1] · Jian Liu[1] · Zhenping Liu[1] · Shangge Liu[1] · Fei Ai[1] · Xiaoqing Zheng[1] ·
Shaohu Ni[2] · Wei Zhang[3]

Abstract Typical large-deformation phenomena of soft rock occurred frequently during the tunneling process in Huangjiazhai Tunnel, Hubei Province, China, including extrusion at the tunnel wall and severe damage of the primary support and secondary lining. To reveal the mechanisms of these anomalies, comprehensive investigations have been undertaken combining engineering, laboratory, and microscopic analyses. Since the monitoring results show that there might be a close relationship between the large deformation phenomena and water infiltration into the tunnel, the water–rock interaction is the research focus in the investigations. The experimental results reveal that the deforming resistance and strength of shales exposed at the excavation face weaken quickly in the first 20 days after the shales have contact with water. The results obtained by mineral composition detection and microstructure observation illustrate the microscopic reasons for the decreasing strength and deforming resistance of the tunnel surrounding rock after water infiltration. The results from in situ geostress tests indicate that as a result of high tectonic stress and low rock strength, the field of Huangjiazhai Tunnel is an extremely high geostress area. By combining analyses from the mechanical and geological perspectives, there are two main reasons for the large deformations in the Huangjiazhai Tunnel: the plastic flow caused by tunnel excavation under high geostress and low rock strength and a hydrated-mechanical coupling process between the shales and water.

Introduction

Highway transportation in mountainous areas is of great importance for local economic development and Tunneling engineering plays a significant role in highway construction in these mountainous regions.

Large deformations of surrounding rock are often encountered during tunnel excavation in rock masses with squeezing characteristics. Generally, the deformation usually lasts from several weeks to several months (Aydan et al. 1996; Brox et al. 1999; Hoek 2001; Meng et al. 2013) or even up to more than 1 year in soft rock tunnels (Yassaghia and Salari-Rad 2005; Wang et al. 2015), often accompanied by the lining cracking and even collapsing. These phenomena are widely observed at relatively shallow depths in soft rocks such as phyllite, mudstone, shale, and siltstone (Aydan et al. 1996). When a tunnel is excavated in a soft squeezing rock, the ground advances slowly into the opening, without visible fracturing or loss of continuity. The continuous inward deformation of the rock may occur together with the separation of rock fragments, or blocks, from the roof and walls of the excavation (Gioda and Cividini 1996). Because of the universality and perniciousness of large deformations in the construction of soft rock tunnels, the squeezing behavior and its mechanisms during tunneling in soft rock layers have aroused much interest among a number of researchers in the past (Wood 1972;

✉ Kang Bian
biankang2002@163.com

1 State Key Laboratory of Geomechanics and Geotechnical Engineering, Institute of Rock and Soil Mechanics, Chinese Academy of Science, Wuhan, Hubei 430072, China

2 Power China Huadong Engineering Corporation Limited, Zhejiang, Hangzhou 310014, China

3 College of Water Conservancy and Civil Engineering, South China Agricultural University, Guangzhou 510642, China

Nakano 1979; Tan et al. 1980; Aydan et al. 1995, 1996; Barla et al. 1995; Kalamaris and Bienawski 1995; Gioda et al. 1996; Kovfiri and Staus 1996; Steiner 1996). Wood (1972) proposed a competency factor, which was defined as the ratio of uniaxial strength of rock to overburden stress to assess the stability of tunnels. Nakano (1979) later used this parameter to recognize the squeezing potential of soft-rock tunneling in Japan. Aydan et al. (1995) and Barla (1995) stated that squeezing was a large, time-dependent deformation that occurred around tunnels and was essentially associated with creep caused by exceeding a shear stress limit. On the basis of surveying and analyzing the similarity of more than 20 squeezing tunnels, Aydan et al. (1993, 1996) proposed that squeezing-type failures tended to occur in soft rock tunnels when several conditions were satisfied, such as a competency factor less than 2 and a tangential strain of the tunnel wall greater than 1%. With an increasing number of soft rock tunnels being constructed, researchers studied large-deformation mechanisms of practical tunnel projects (Khanlari et al. 2012; Meng et al. 2013; Agan 2016). Among them, Meng et al. (2013) summarized three factors inducing large deformations in Zhegu Tunnel, situated on the Sichuan-Tibet Highway: the plastic flow of soft rock, shear sliding of wedges, and bending of thin-layered soft rock.

Over the past several decades, a number of researchers have studied the large deformations in squeezing tunnels, especially the extent of the plasticity zone (Anagnostou 1993; Duncan 1993; Yassaghia et al. 2005; Sterpi et al. 2009; Meng et al. 2013; Wang et al. 2015; Agan 2016). Many studies (Brox et al. 1999; Dalgic et al. 2002; Bizjak and Petkovsek 2004; Khanlari et al. 2012; Wang et al. 2015) have focused on the large-deformation mechanisms from the perspective of either mechanics or geology. To reveal the mechanisms of large deformations in a squeezing tunnel, integrated analyses of the mechanical and geological methods are usually essential. However, investigations of the causes triggering squeezing in soft rock tunnels are normally not comprehensive in the existing research; few studies have researched this problem by combining engineering, laboratory, and microscopic analyses. Because of the various geological conditions in different tunnels, each tunnel has distinct reasons underlying the observed squeezing problems. To intrinsically reveal the causes of large deformations for a specific tunnel, comprehensive investigations must be carried out. It has been demonstrated that squeezing can be controlled effectively by installing yielding supports (Hoek and Guevara 2009; Cantieni and Anagnostou 2009; Barla et al. 2011; Aksoy et al. 2012), and the use of simple sliding joints in steel sets has proven to be a very effective means for providing emergency support in the event of a tunnel collapse close to the face (Hoek et al. 2009). If the permissible deformations are known beforehand, measures such as the design of steel fiber reinforced shotcrete (SFRS) may be used to solve the squeezing problem (Singh et al.

2007). Adopting higher-capacity segmental lining systems will extend the operational possibilities for Tunnel Boring Machine (TBM) in squeezing rock (Mezger et al. 2017).

Water-weakening effects are widely believed to be an important factor contributing to large deformations in soft rock tunnels, and most of the past relevant research (Van Eeckhout 1976; Alm 1982; Hadizadeh and Law 1991; Erguler et al. 2009; Yilmaz 2010; Duda and Renner 2012; Jiang et al. 2014) has concentrated on the mesoscopic mechanisms and mechanical properties of soft rock influenced by water. However, little research has investigated the relationship between the mesoscopic mechanisms of soft rock and the macroscopic deformation behavior of a tunnel with water infiltration. In this paper, we study the interaction between the hydration effect of shales and the deformation behavior of tunnel rock. The coupling process continuously cycles and finally induces the large deformation and even failure of the tunnel.

In this paper, to reveal the mechanism of large-deformation phenomena during tunneling in Huangjiazhai Tunnel, comprehensive investigations have been undertaken by combining engineering, laboratory, and microscopic analyses. The large deformation in Huangjiazhai Tunnel has two main reasons: the plastic flow caused by tunnel excavation under high geostress and low rock strength and the hydrated-mechanical coupling process between shales and water.

Topographic and geological conditions

Location and topographic conditions

Huangjiazhai Tunnel is one of the 29 tunnels of the Macheng-Zhuxi Highway, which is located in the north-west of Hubei Province in Central China. The owner of Huangjiazhai Tunnel is Hubei Provincial Communications Investment Group Co., Ltd., a wholly state-owned company funded by the Government of Hubei Province. The tunnel was constructed between 29 May 2013, and 25 December 2015, and the construction period lasted for nearly 2.5 years. Designed as a long, separated tunnel, Huangjiazhai Tunnel has a maximum buried depth of 270 m and a length of 1437 m. Both tunnels are of 12.4 m width and 9.9 m height, and an end-wall tunnel portal was chosen. The tunnel sites are mainly hilly areas, and there are also some valleys and terraces.

Lithology

The principal stratum at the construction site of the Huangjiazhai Tunnel is Silurian shale belonging to the Sllm Group (S_1l). Quaternary residual gravelly soil (Q_4^{el+dl}) constitutes the covering layer of this area. Geological explorations via boreholes drilled at the tunnel route show that three layers divide the ground surface to the bottom: gravelly soil, heavily

weathered shale and moderately weathered shale. The topographic map and geological profile of Huangjiazhai Tunnel are shown in Figs. 1 and 2. The estimated rock mass classification systems of Huangjiazhai Tunnel are shown in Table 1.

The gravelly soil, which is made up of shale fragments and small amounts of clay, displays a yellow to brown color. The diameter of these shale pieces ranges from 2 to 8 cm, and the soil thickness at the entrance to the tunnel varies between 1.7 and 14.8 m. The heavily weathered shale has a pelitic texture, with thin- and medium-layered structures and well-developed joints. The layer thickness of heavily weathered shale usually ranges from 10.2 to 26.4 m, and the cores are mostly fragmentized. The moderately weathered shale is medium-jointed, with a depth generally from 10 to 20 m. The cores drilled from the boreholes of the three layers are shown in Fig. 3.

Geological structure

According to data on the regional structure of Hubei Province, Huangjiazhai Tunnel is located at the intersection of the third uplifted zone of a Neocathaysian system and the west reflex-arc of the Huaiyang epsilon-type structure. A world-class fault, Qingfeng Fault, is located in the north of Huangjiazhai Tunnel. East-west folded belts and fractured zones of the west reflex-arc of the Huaiyang epsilon-type structure run through the tunnel sites. A north–north-east (NNE) tectonic belt and a north–north-west (NNW) fractured zone, both of which belong to the Neocathaysian system, overlay the epsilon-type structure.

Hydrogeology

The groundwater at the tunnel site, which is composed of fissure water at bedrock and pore water at the loose bed of Quaternary, is supplied by the infiltration of atmospheric precipitation. The annual average rainfall is 800–1200 mm at the tunnel site, mostly in summer, when the south-east monsoon carries rainwater into the inland provinces.

Large-deformation phenomena during tunneling and monitoring situation

Large-deformation phenomena during tunneling

The New Austrian Tunneling Method (NATM) was applied in the construction of Huangjiazhai Tunnel. The bench-cut method was utilized at Chainage K60 + 860–K60 + 980, K61 + 140–K61 + 240 and K61 + 320–K61 + 440 in the right tunnel, and it was applied at Chainage ZK60 + 830–ZK60 + 945, ZK61 + 166–ZK61 + 196 and ZK61 + 310–ZK61 + 603 in the left tunnel, with a total length of 778 m. In the residual sections where the rock masses were considered soft and fragmentized, the ring cut method (Hisatake et al. 2009; Hisatake et al. 2012) was adopted. The initial supports in the tunnel were combinative technologies, including ductile grouting, steel arch, reinforcing mesh, and shotcrete. Reinforced concrete was adopted as the secondary lining. The details of the construction procedure and supports for the ring cut method are shown in Fig. 4.

Continuously exposed at the excavation surface during the tunneling process, most of the rock masses were fragmentized, thin-layered, and jointed (Fig. 5). The groundwater developed at several sections in Huangjiazhai Tunnel (e.g., Chainage ZK61 + 977–ZK62 + 010, ZK61 + 603–ZK61 + 624, ZK61 + 203–ZK61 + 196, ZK61 + 166–ZK61 + 156, ZK61 + 122–ZK61 + 112, ZK61 + 085–ZK61 + 052, ZK61 + 052–ZK61 + 036, ZK60 + 690.5–ZK60 + 707,
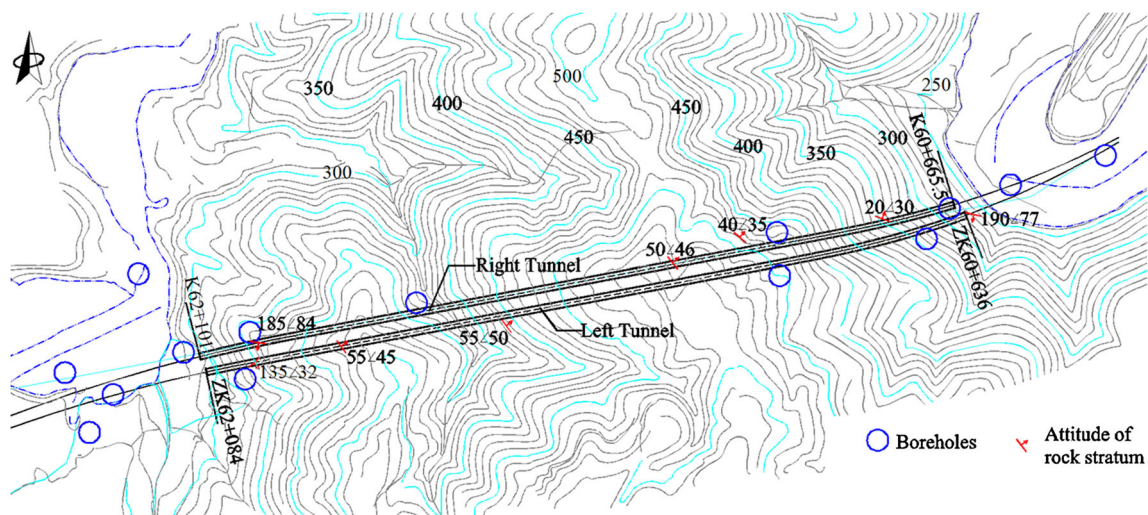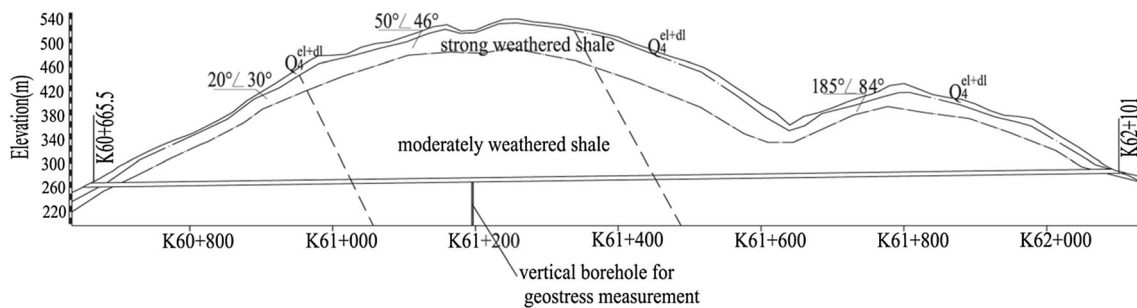

Fig. 1 Topographic map of Huangjiazhai Tunnel

Fig. 2 Geological profile of Huangjiazhai Tunnel

ZK60 + 945–ZK60 + 980.6, and ZK60 + 726.5–ZK60 + 747.1 in the left tunnel, and Chainage K60 + 803–K60 + 784, K61 + 132–K61 + 112, K61 + 072–K61 + 055, K60 + 720–K60 + 745, and K60 + 745–K60 + 763 in the right tunnel). Among these tunnel sections, the groundwater at Chainage K61 + 132–K61 + 112 and K61 + 072–K61 + 055 was the most abundant, as shown in Fig. 6. Collapse occurred occasionally in Huangjiazhai Tunnel. For instance, on 1 September 2015, a collapse occurred at the excavation surface at Chainage K60 + 762.8 in the right tunnel, as shown in Fig. 7a. When the collapse occurred, construction at the excavation

surface was halted. The steel arches between Chainage K60 + 733 and K60 + 734.2 had to be replaced at that time; the primary supports of these sections were chiseled off by the workers. First, some of the rock fragments were seen to slip from the left sidewall and crown; as time passed, the number of rock fragments increased rapidly, and collapse at the excavation surface was induced afterwards. Typical large-deformation phenomena of soft rock occurred frequently, such as extrusion of the tunnel wall (Chainage K60 + 745–K60 + 763, Fig. 7b), damage of the primary supports (Chainage ZK60 + 980.6–ZK60 + 945, Fig. 7c), and surface peeling of the secondary lining (Chainage K61 + 026–K61 + 014, Fig. 7d). According to the statistics, a special alteration of rock mass grade occurred 27 times in constructing Huangjiazhai Tunnel, resulting in a dramatic increase in the project costs and a delay in the tunnel construction.

Table 1 The estimated rock mass classification systems in Huangjiazhai Tunnel

Chainage	Length /m	RMR
K60 + 666–K60 + 750	84.5	16
ZK60 + 636–ZK60 + 720	84	
K60 + 750–K60 + 860	110	31
ZK60 + 720–ZK60 + 830	110	
K60 + 860–K60 + 980	120	44
ZK60 + 830–ZK60 + 980	150	
K60 + 980–K61 + 060	80	32
ZK60 + 980–ZK61 + 010	30	
K61 + 060–K61 + 140	80	17
ZK61 + 010–ZK61 + 140	130	
K61 + 140–K61 + 170	30	35
ZK61 + 140–ZK61 + 170	30	
K61 + 170–K61 + 240	70	32
ZK61 + 170–ZK61 + 240	70	
K61 + 240–K61 + 320	80	27
ZK61 + 240–ZK61 + 310	70	
K61 + 320–K61 + 440	120	43
ZK61 + 310–ZK61 + 430	120	
K61 + 440–K61 + 700	260	34
ZK61 + 430–ZK61 + 720	290	
K61 + 700–K61 + 890	190	31
ZK61 + 720–ZK61 + 900	180	
K61 + 890–K62 + 020	130	33
ZK61 + 900–ZK62 + 000	100	
K62 + 020–K62 + 101	81	15
ZK62 + 000–ZK62 + 084	84	

RMR rock mass rating

Monitoring situation

The monitoring results provide quantitative data to analyze the real situation during the tunneling process. The horizontal displacement of Huangjiazhai Tunnel was measured with tape extensometers, which measure the distance between reference points (hooks) bolted on the tunnel wall. The accuracy of such measurements is typically ±0.2 mm for distances up to 10–15 m (Kavvadas 2005; Walton et al. 2014).

The vertical displacement of Huangjiazhai Tunnel was measured with total station. Total station surveying uses optical reflectors that are installed around the tunnel profile (usually at five to seven points) and a stable reference point that is outside the zone of convergence to measure deformations. The total station must be moved progressively forward from the location of the stable reference points to the tunnel excavation surface as the tunneling progresses. Total stations have an accuracy of about ±2.5 mm over 100 m for tunneling applications (Kavvadas 2005; Walton et al. 2014).

Figure 8 shows the monitoring results of displacement at two typical sections of Huangjiazhai Tunnel. During the monitoring period of 27 days, the maximum accumulative horizontal displacement exceeded 500 mm, and the maximum velocity of horizontal convergence reached 60.6 mm/day. Compared

Fig. 3 Cores drilled from boreholes of three strata at Huangjiazhai Tunnel: (*a*) gravelly soil; (*b*) heavily weathered shale; and (*c*) moderately weathered shale

with the horizontal convergence, the vertical displacement was slightly smaller; however, the maximum accumulative vertical displacement reached 304 mm. After monitoring for 5 or 6 days, the deformation velocity decreased compared with that in the earlier days; nevertheless, the velocity was still great. Throughout the monitoring period, both the horizontal and vertical deformations at the monitored sections showed no possibility of convergence. The deformation in Huangjiazhai Tunnel had the properties of large magnitude, high velocity, and long duration. Since the ground displacements that occurred immediately after tunnel excavation could not be monitored, the laser measuring instrument was also utilized in this tunnel section. The results showed that the actual horizontal deformation of the sections exceeded 800 mm. In this case, the originally designed contour lines of the tunnel had been encroached. The primary supports at these large-deformation parts, including the distorted steel arches and cracked shotcretes, together with the squeezing rock masses, were chiseled off meter by meter. Immediately after chiseling, new steel arches were installed and the new shotcrete-bolting-mesh supports were applied. The above cycles were repeated until all of the large deformations were repaired.

Figure 9 shows the monitoring results of contact pressure between the primary support and secondary lining at Chainage ZK61 + 746 in Huangjiazhai Tunnel. During the observation period, the contact pressure increased quickly in the initial month; thereafter, the velocity of pressure increment gradually decreased and became stable. The pressure at the crown remained unchanged from early September 2014, and the value at the tunnel wall maintained a continuously increasing trend until the middle of October 2014. In general, the pressure was higher at the tunnel wall than at the crown, and the maximum contact pressure occurred at the right tunnel wall, which was in excess of 0.68 MPa.

According to former research (Zhu et al. 2007; Yang et al. 2014), shale is considered a type of rock with typical rheological properties. The experimental results from the direct-shear creep tests showed that the shear modulus, shear strain, and shear stress all have non-linear relationships with time, and a rheological model has been developed to describe the rheological characteristics of shales (Yang et al. 2014). Other experimental research showed that the axial and lateral creep curves of shale specimens exhibit the attenuation creep stage under a relatively low stress state. The rheological constitutive equation was obtained via the parametric regression of an Hooke-Kelvin (H-K) three-component model (Zhu et al. 2007). The above observed deformation characteristics and contact pressure seem to be explained by the typical rheological property of the shale in Huangjiazhai Tunnel. However, considering the buried depth of the large-deformation regions (generally approximately 150–200 m), it is still
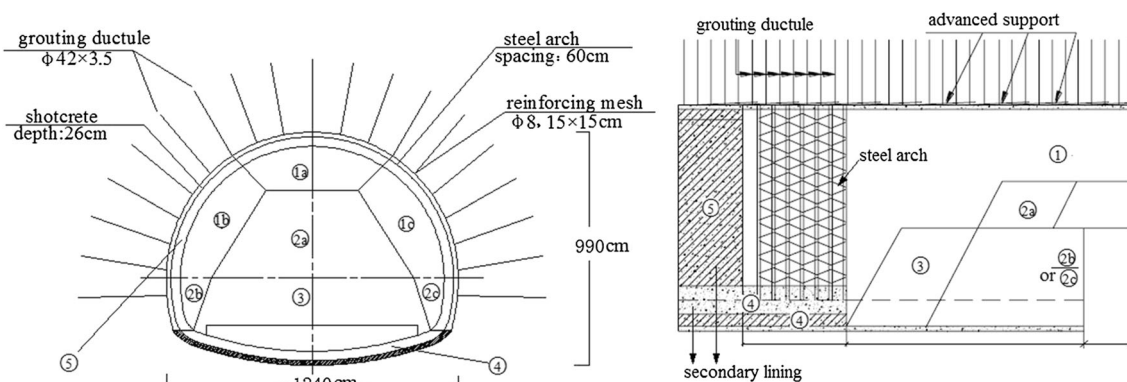
Fig. 4 Details of tunnel construction procedure and supports for the ring cut method
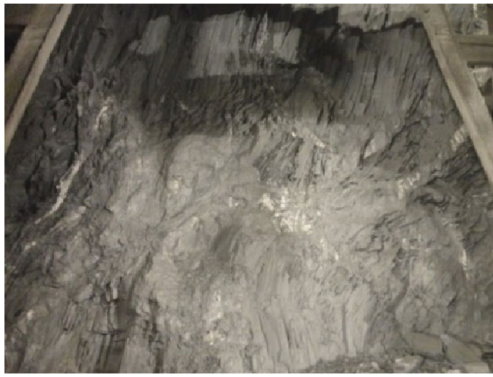
Fig. 5 Rock masses at the excavation surface at Chainage K61 + 931 in Huangjiazhai Tunnel

difficult to understand such large deformations and high contact pressures. It was found that the tunnel deformed intensively during continuous rainy days; on the days without rain, the occurrence of severe deformations decreased dramatically. Consequently, it appeared that there might be close relationships between the large deformation and water infiltration into the tunnel.

Investigations of the mechanism of large deformations in Huangjiazhai Tunnel

Large-deformation phenomena in a soft rock tunnel could be induced by several potential causes. The geological conditions are considered to be essential causes inducing large-deformation problems in tunnels (Brox and Hagedorn 1999; Yassaghia et al. 2005; Sterpi and Gioda 2009; Khanlari et al. 2012; Meng et al. 2013; Agan 2016). The strength–stress ratio (SSR), which can be defined as the ratio between the uniaxial compressive strength of rock mass σ_{cm} and the in situ stress P_0, is widely recognized as a factor that describes the extent of rock squeezing (Hoek et al. 2000; Hsiao et al. 2009). The mechanical properties of rock masses and geostress levels

are important factors inducing large-deformation phenomena in tunnels. Previous studies (Tan and Kang 1980; Anagnostou 1993; Erguler and Ulusay 2009; Meng et al. 2013) have indicated that rock swelling due to clay material encountering groundwater is one of the most important factors in large deformation during tunneling. Therefore, the mineral composition of rock masses and groundwater are also potential factors that trigger squeezing in the tunnel. Since the monitoring results show that there might be a close relationship between the large deformation and water infiltration, the water–rock interaction was the research focus of the investigations. Therefore, in addition to a geostress test, a series of laboratory experiments was carried out, including uniaxial compression tests, microstructure observations of shale under different immersion times, and mineral composition detection, to reveal the mechanisms of such anomalies during the construction of Huangjiazhai Tunnel.

Uniaxial compression tests for different immersion times

Rock samples obtained from the intact shale inside Huangjiazhai Tunnel were processed into Φ50 mm × 100 mm cylindrical specimens. Most of the samples were prepared according to the saturated standard, which was based on "GB/T 50266–2013 (2013) (Standard for test methods of engineering rock mass)", a Chinese national standard, in which the procedure to saturate the rock specimens was described. The immersion time was 2, 15, 30, 50, 70, and 90 days ('immersion time' refers to the time elapsed since immersion of the specimens). First, the specimens were put into a trough, and water was injected into one-quarter of the specimen's height. After 2 h, water was injected into half of the specimen's height, and another 2 h later, to three-quarters of the specimen's height. After 6 h, the specimens were fully submerged. The uniaxial compression tests of the dry and saturated specimens were conducted on the Rock Mass Testing System (RMT), and the mechanical parameters of rock specimens with different
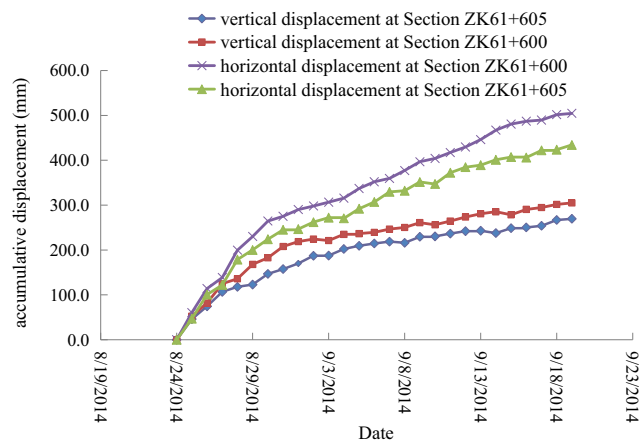
Fig. 6 Groundwater in Huangjiazhai Tunnel

Fig. 7 Anomalies in Huangjiazhai Tunnel during the tunneling process: (*a*) collapse inside the tunnel; (*b*) squeezing of the sidewall; (*c*) damage of the primary support; and (*d*) surface peeling of the secondary lining
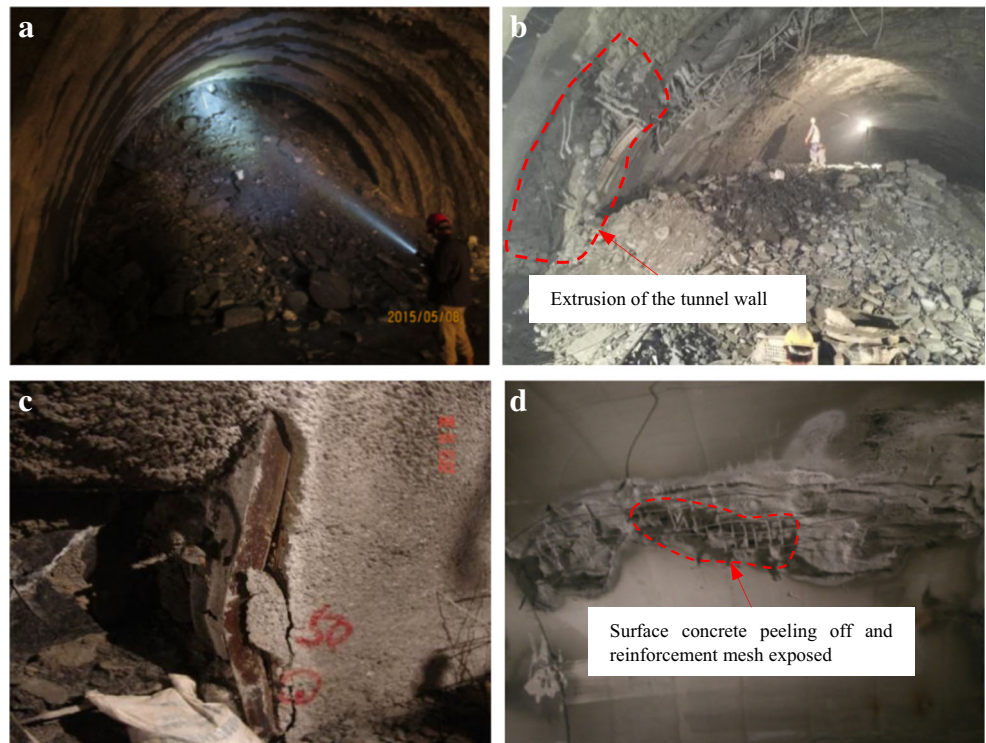
immersion times are shown in Table 2. Figure 10 shows the fitting curves of the elastic modulus and immersion time of rock specimens, and Fig. 11 shows the curves of the uniaxial compressive strength and immersion time. The uniaxial compressive strength and elasticity modulus of the rock samples gradually declined along with the increase of immersion time, which indicated that the deforming resistance and strength of shales weaken with an increase of time in a wet environment. After the saturated status had persisted for 90 days, the uniaxial compressive strength and elasticity modulus of the rock samples were reduced by 62% and 56% compared with the values in the dry state.

The relationship between the uniaxial compressive strength and immersion time is described by the following expression (Eq. 1):

$$\sigma_c = 60.45 - 8.82\ln t \quad (t > 1) \qquad (1)$$

where σ_c is the uniaxial compressive strength of shale (MPa) and t is the immersion time (day).

Equation 1 shows that the uniaxial compressive strength had a negative logarithmic relationship with immersion time. The uniaxial compressive strength of shale declined quickly in the initial 20 days. With an increase in the immersion time, the rate of reduction decreased. When the saturated status had

Fig. 8 Curves of displacement and time at two sections of the tunnel
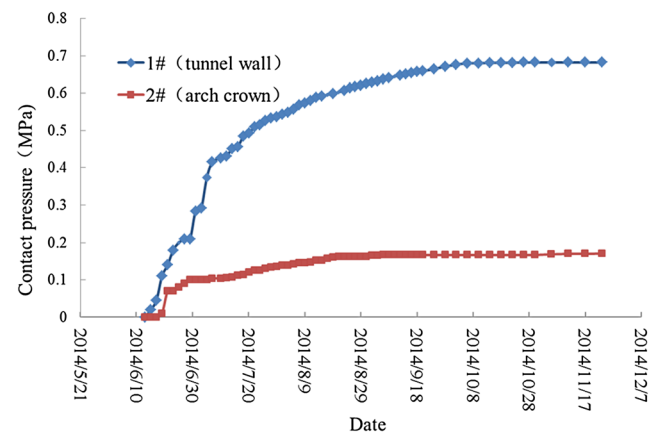
Fig. 9 Curves of contact pressure and time at Chainage ZK61 + 746

Table 2 Mechanical parameters under different immersion times of the rock specimens

Immersion time (days)	Elastic modulus (GPa)	Possion's ratio	Uniaxial compressive strength (MPa)
0	27.38	0.295	56.85
2	25.67	0.312	52.66
15	20.90	0.343	41.32
30	17.59	0.355	30.23
50	13.55	0.388	23.15
70	12.36	0.392	22.25
90	11.40	0.412	21.54

Fig. 11 Curves of uniaxial compressive strength and immersion time for rock specimens

persisted for 50 days, the uniaxial compressive strength had become approximately stable.

Similarly, the relationship between the elasticity modulus and immersion time could be described by the following fitting expression (Eq. 2):
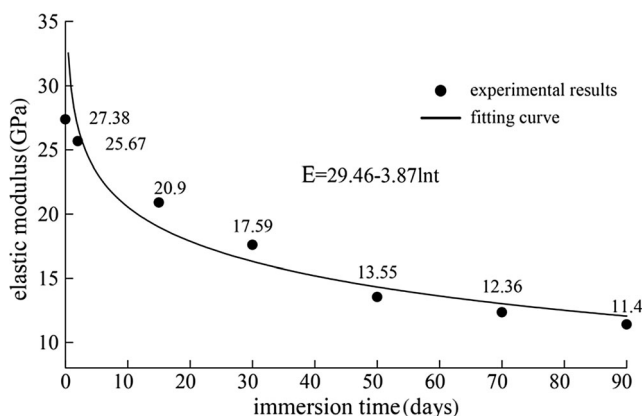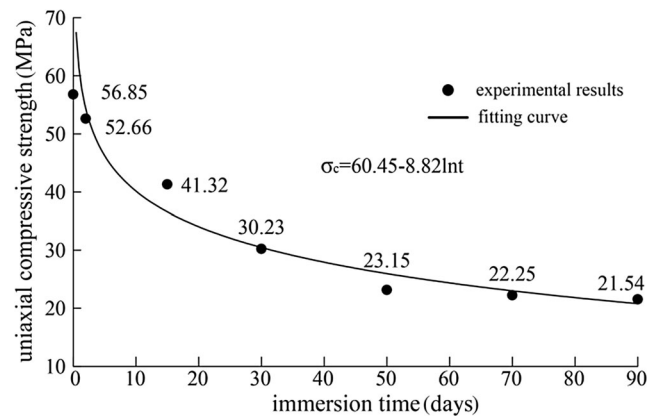
$$E = 29.46 - 3.87\ln t \quad (t > 1) \tag{2}$$

where E is the elasticity modulus of shale (GPa) and t is the immersion time (day).

It is important to note that to achieve the experimental standard, the rock samples were collected from the shale with the best integrity and highest strength. However, most of the rock masses in Huangjiazhai Tunnel were actually fragmentized, thin-layered, and jointed. Thus, the mechanical parameters in Table 2 are generally much larger than those of the rock masses exposed at the excavation surface of tunnel.

Mineral composition detection

The mineral compositions of the rock samples can be quantitatively identified by X-ray diffraction (XRD) analysis, and

the tests were conducted on a D8 Advanced X-ray diffractometer. The shale samples, taken from eight different positions at Huangjiazhai Tunnel, were ground to powder. The scanning angle was between 3 ° and 50 °, and the scanning velocity was 5 °/min. The voltage and current were 40 kV and 80 mA, respectively. The results showed that the shale samples were composed primarily of chlorite, quartz, muscovite, and albite, with a small amount of calcite, as shown in Table 3 and Fig. 12. Among all of the components, the chlorite accounted for the highest amount, ranging from 31.12% to 42.66%, followed by the albite, with a content of 11.35–36.28%. The content of muscovite was relatively fixed and was approximately 20%.

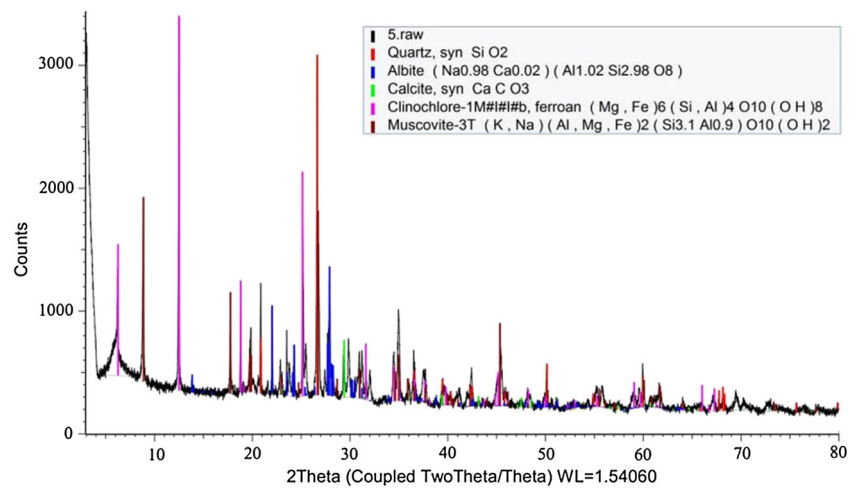## Microstructure observation of shale for different immersion times

The microstructural features of the different minerals contained in rock samples, including the type of minerals and crystal morphology, can be observed using scanning electron microscopy (SEM) techniques. A micrograph of a dry

Fig. 10 Curves of elastic modulus and immersion time for rock specimens

Table 3 Mineral content of shale in Huangjiazhai Tunnel

Sample number	Mineral content (%)				
	Calcite	Albite	Quartz	Muscovite	Chlorite
1	5.80	12.36	31.25	17.03	33.56
2	4.02	12.27	33.10	19.48	31.12
3	3.63	14.93	20.37	22.04	39.02
4	0.74	12.06	21.67	23.75	41.78
5	3.28	21.70	11.35	21.02	42.66
6	–	16.77	30.78	19.09	33.36
7	0.84	17.30	34.72	14.91	32.23
8	0.96	10.01	36.28	17.72	35.03

Fig. 12 Mineral compositions of the shale samples from Huangjiazhai Tunnel

sample is shown in Fig. 13a, and the microstructures of shale for different immersion times are listed in Fig. 13b–d. Micrographs with different magnifications are shown in Fig. 14, with an immersion time of 50 days.
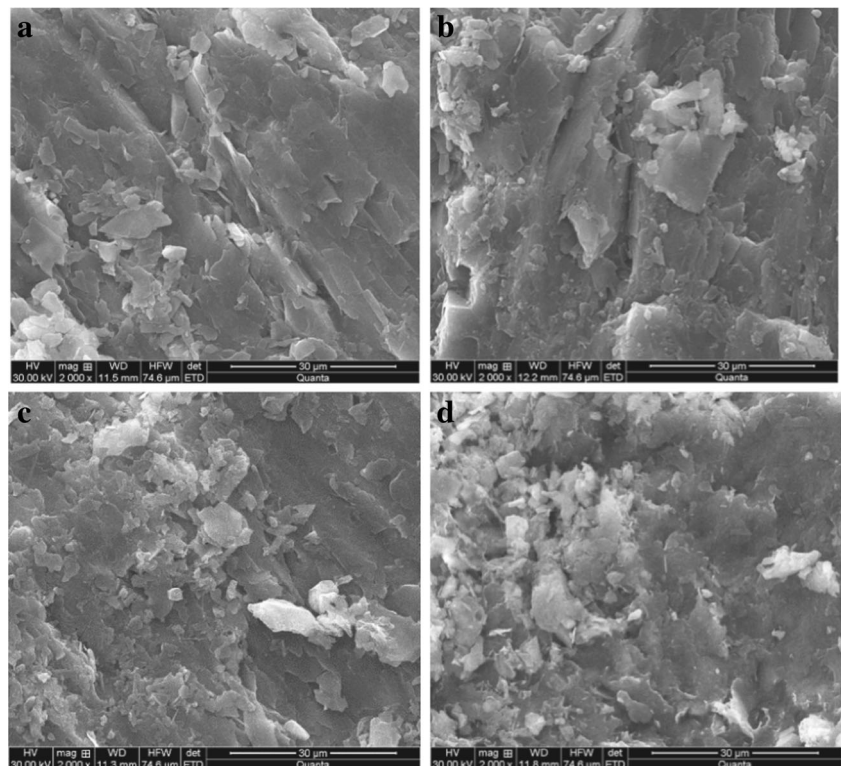
In dry conditions, the chlorite crystals presented laminar-structure aggregate morphologies, with a diameter of approximately 50 μm. The microstructures were compact, with few micro-pores and micro-cracks. The mineral particles were mostly bonded in a face-to-face contact style.

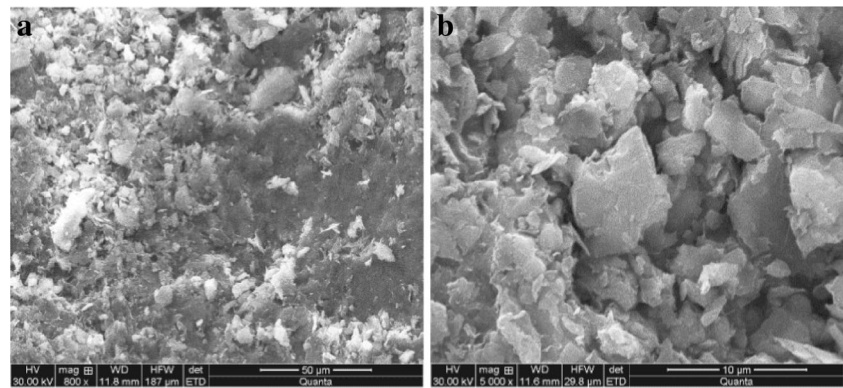When the samples had been saturated for 2 days, the laminar structures of chlorite began peeling off as a result of hydration, with a diameter of approximately 8 μm for a peeling particle. At this stage, the face-to-face contact remained the primary style; however, as more mineral particles separated from the laminar structure, the number of point-to-face contacts increased. The compact laminar structures became loose, and the edges of the structures gradually fragmentized. A large number of micro-pores appeared among the mineral particles.

After the saturated status had lasted for 20 days, the mineral particles increasingly peeled off, and the cementation among mineral particles was weakened. In this case,

Fig. 13 Micrographs of shale for dry and saturated conditions (magnification: 2000): (*a*) dry; (*b*) saturated for 2 days; (*c*) saturated for 20 days; (*d*) saturated for 50 days

the microstructures of the samples were less compact, and the scales of micro-pores and micro-cracks inside the shale quickly expanded. The peeling particles scattered into smaller ones, with a diameter of approximately 3 μm, filling in the micro-pores and micro-cracks. The flocculent microstructures emerged in this stage, making the shale much more fragmentized. The dominant combination style gradually changed from face-to-face to point-to-face contact.

After the saturated status had lasted for 50 days, an increasing number of flocculent microstructures had appeared due to continuous hydration, leading to increased damage to the original cementation among mineral particles. At this stage, the compact laminar structures mostly became porous loose ones, and the dominant combination style became point-to-face.

This analysis illustrates the reasons for the decrease of strength and deforming resistance of tunnel rock after water infiltration from the micro perspective.

Geostress test

The geostress test was carried out to assess the geostress level at the field of Huangjiazhai Tunnel. The vertical borehole for geostress measurement, with a depth of 50 m, was located at Chainage K61 + 195 in the right tunnel (Fig. 15), and the buried depth of measurement was 260 m. The hydraulic fracturing method, which has been widely used to measure geostress (Matsunaga et al. 1989; Kuriyagawa et al. 1989; Hayashi and Ito 1993; Haimson and Cornet 2003), was applied at Huangjiazhai Tunnel. The in situ test results are listed in Table 4. The hydraulic fracturing test procedure is as follows:

(1) The borehole with a depth of 50 m along the vertical direction was drilled, and continuous cores were extracted.
(2) The test interval was sealed off by positioning the straddle packer at the planned depth, and the packers were pressurized to a typical level of 3 MPa.
(3) The test interval was pressurized for an initial qualitative permeability inspection (slug test).
(4) The interval pressure was raised to maintain a constant, predetermined flow rate.
(5) Upon reaching breakdown pressure, pumping was stopped.
(6) After the pore pressure had reached its original value, i.e., after waiting for a few minutes, the above

pressurization was repeated and cycled three times, using the same flow rate.

(7) Finally, both the test interval and the packer pressure were vented to allow the packers to deflate.

As shown in Table 4, within the depth range of geostress measurement, the maximum horizontal principal stress at the borehole was 14.60 MPa. The results indicated that the maximum principal stress and the second principal stress were both horizontal stresses and that only the minimum principal stress was in the vertical direction. The lateral pressure coefficient, i.e., the ratio of the maximum horizontal principal stress and the vertical stress, reached nearly 1.8, indicating that the tectonic stress was the primary composition of geostress at the tunnel site. Consequently, it was concluded that the site had experienced intense tectonic movements in geological history, which could also be verified by the littery attitude of exposed rock masses at the excavation surface.

Mechanism of large deformation in Huangjiazhai Tunnel

The mechanisms of large deformation in Huangjiazhai Tunnel can be attributed to a number of reasons, both geological and mechanical. The main inducing factors are summarized in the following sections.

Plastic flow of rock masses induced by tunnel excavation under high geostress and low rock strength

According to previous research (Anagnostou 1993; Meng et al. 2013), excavation-induced plastic deformation is considered one of the most important factors resulting in squeezing in soft rock tunnels. The deformation in plastic flow will appear to different extents, moderate or severe, depending on the magnitude of geostress and rock strength. A quantitative evaluation of the rock strength and geostress magnitude around the in situ test hole at Huangjiazhai Tunnel is given in this section, utilizing the loading factors, e.g., σ_{cm}/P_0 and R_c/σ_{max}.

The rock mass rating (RMR) system was initially developed by Bieniawski (1974, 1989) on the basis of his experiences in shallow tunnels. According to the geological exploration data shown in Table 1, the value of RMR at the geostress test areas of Huangjiazhai Tunnel (Chainage K61 + 195) is 32.

Over the past several decades, based on the rock mass classification system, many empirical equations for calculating the strength of rock mass (σ_{cm}) have been proposed. The most widely used equations and the results of σ_{cm} at the geostress test areas are listed in Table 5. In these equations, σ_{ci}, the strength of intact rock (MPa), is 56.85 MPa at the geostress test areas, as shown in Fig. 11.

On the basis of the equations in Table 5, the average value of σ_{cm} at the drilling hole is 3.2 MPa. The in situ stress P_0 at the geostress test area is 14.6 MPa. The SSR, defined as σ_{cm}/P_0 (Wood 1972; Nakano 1979; Hoek and Marinos 2000), is 0.22 at Chainage K61 + 195, which is less than the cut-off value of σ_{cm}/P_0 (0.25; between moderately squeezing rock and severely squeezing rock) (Hsiao et al. 2009). Consequently, the rock masses at the abovementioned area of Huangjiazhai Tunnel are considered to be severely squeezing rock.

In "GB/T 50218–2014 (2014) (Standard for Engineering Classification of Rock Mass)", a Chinese national standard describing the classification of engineering rock masses, the factor of R_c/σ_{max} is adopted to evaluate the grade of the initial stress field. R_c/σ_{max} is defined as the ratio of uniaxial compressive strength of saturated rock to maximum principal stress. Similar to choosing 0.25 as the cut-off value of σ_{cm}/P_0 to differentiate moderately squeezing rock and severely squeezing rock (Hsiao et al. 2009), 4 is chosen to be the cut-off value of R_c/σ_{max} to differentiate high geostress from extremely high

Table 4 Results of the geostress test in vertical boreholes at Huangjiazhai Tunnel

Depth (m)	Maximum horizontal principal stress (σ_H [MPa])	Minimum horizontal principal stress (σ_h [MPa])	Vertical stress (σ_v [MPa])	Direction of maximum horizontal principal stress
18	2.44	2.14	7.23	/
22	6.41	4.30	7.33	/
26	13.20	7.01	7.44	/
30	12.61	6.56	7.54	/
37	11.90	6.56	7.72	/
39	14.33	7.85	7.77	NE8°
41	14.60	7.86	7.83	NE10°

NE north-east

Table 5 The empirical equations and results of strength of rock mass (σ_{cm}) at the geostress test areas

Researcher	Equation	σ_{cm} (MPa)
Kalamaris and Bieniawski (1995)	$\sigma_{cm} = \sigma_{ci}\exp\left[\frac{RMR-100}{24}\right]$ (MPa)	3.34
Sheorey (1997)	$\sigma_{cm} = \sigma_{ci}\exp\left[\frac{RMR-100}{20}\right]$ (MPa)	1.90
Trueman (1998)	$\sigma_{cm} = 0.5\exp(0.06RMR)(MPa)$	3.41
Aydan and Dalgic (1998)	$\sigma_{cm} = \frac{RMR}{RMR+6(100-RMR)}\sigma_{ci}(MPa)$	4.13

geostress by summarizing the geological data from a number of projects. An area is considered to bear extremely high stress when R_c/σ_{max} is less than 4.

Based on the results of geostress tests and laboratory experiments, the maximum value of R_c/σ_{max} is 3.89 at the bottom of the geostress test hole. Consequently, it indicates that although the maximum buried depth (270 m) of the tunnel is not too large, the geostress test area of Huangjiazhai Tunnel is still considered an extremely high stress area due to the high tectonic stress and low rock strength.

According to the Mohr-Coulomb criterion, the yielding of rock mass has close relationships with both the deviator stress and the rock strength. The adjusted deviator stress after excavation in a high stress case is obviously higher than that in a low stress case, which leads to the rock fracture propagation and further accelerates the deformation and failure of rock masses. Compared with the case of high rock strength, rock masses with low strength yield more easily, resulting in a larger deformation of plastic flow. High geostress and low rock strength are important factors in the large deformation at Huangjiazhai Tunnel.
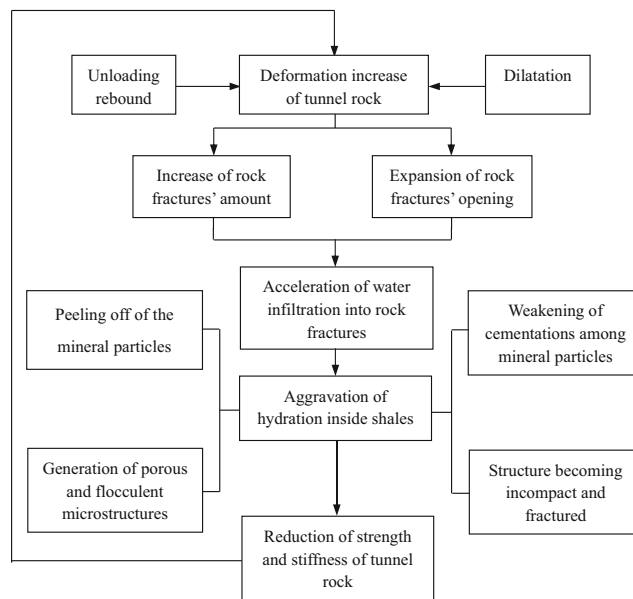
Hydrated-mechanical coupling process in rock masses

The results of laboratory experiments show that the uni-axial compressive strength and elasticity modulus of the rock samples are gradually reduced along with an increase in the immersion time, following a negative logarithmic relationship. This result indicates that the deforming resistance and strength of shales exposed at the excavation surface are quickly weakened in the initial 20 days after the shales contact water. From the mechanical perspective, this is also why Huangjiazhai Tunnel deforms intensively during the continuous rainy days.

The results of XRD analysis indicate that the chlorite and muscovite account for a large proportion of the mineral composition of shale. According to previous research (Teng et al. 2010), both have the characteristics of hydro-expansiveness. For muscovite, the spacing of the crystal layer increases by

0.285% after saturation, and the increased proportion of expansive force reaches 124.4%; for chlorite, the respective values are 0.047% and 111.8%. Another study (Zhu 1996) showed that the water molecules are adsorbed on the surface of the chlorite particles, after which the polarized layers of water molecules form. Through continuous water absorption, the layers of water molecules gradually thicken, causing the volume expansion of chlorite. Since the volume expansion is heterogeneous, differential expansion stresses appear inside the chlorite, inducing the dissolution of argillaceous cementation; consequently, the shales gradually fragment.

The hydrated-mechanical coupling process in rock masses is shown in Fig. 16. Due to the effects of dilatancy and unloading rebound of rock masses in the process of tunnel excavation, the number of rock fractures increases, and the fracture apertures increase in size. Groundwater continuously infiltrates into the rock mass along the rock fractures, thus accelerating the hydration process inside the shales. As time passes, the chlorite and muscovite at the surface of shales gradually swell and peel off, and more porous and flocculent microstructures appear at the peeling particles, making the structures increasingly incompact and fragmentized. The cementations among mineral particles are gradually dissolved, and the cohesion and stiffness of shales decrease, thereby inducing larger deformations of rock masses after excavation. As a result, more rock fractures expand, and more surfaces contacting water are exposed inside the rock masses, thus aggravating the hydration action. The above cycles repeat and finally induce the large deformation and even failure of the tunnel.

Fig. 16 Hydrated-mechanical coupled process in rock masses of the Huangjiazhai Tunnel

Conclusions

Severe deformation phenomena occurred frequently during tunneling in Huangjiazhai Tunnel in Hubei Province, China. To determine the mechanisms of such anomalies, comprehensive engineering, laboratory, and microscopic investigations were conducted, including geostress tests, uniaxial compression tests, microstructure observations of shale with different immersion times, and mineral composition detection.

The experimental results show that the uniaxial compressive strength and elasticity modulus of the rock samples decrease gradually along with an increase in the immersion time, following a negative logarithmic relationship. When the saturated status lasts for 90 days, the uniaxial compressive strength and elasticity modulus of the rock samples are reduced by 62% and 56% compared with the values under dry conditions. This indicates that the deforming resistance and strength of shales exposed at the excavation surface of Huangjiazhai Tunnel are quickly weakened in the initial 20 days after the shales contact water. The mineral composition detection and microstructure observation results illustrate the reasons for the decrease in strength and deforming resistance of tunnel rock masses after water infiltration.

According to the results of in situ geostress tests, the maximum horizontal principal stress at the borehole in Huangjiazhai Tunnel is 14.60 MPa. Although the maximum buried depth (270 m) of the tunnel is not too large, considering the high tectonic stress and low rock strength, the geostress test area of Huangjiazhai Tunnel can be considered an extremely high stress area.

By combining engineering, laboratory, and microscopic analyses, the large deformation at Huangjiazhai Tunnel can be attributed to two primary triggering factors: the plastic flow induced by tunnel excavation under high geostress and low rock strength and the hydrated-mechanical coupling process in the shales.

References

Agan C (2016) Prediction of squeezing potential of rock masses around the Suruc water tunnel. Bull Eng Geol Environ 75:451–468

Aksoy CO, Ogul K, Topal I, Ozer SC, Ozacar V, Posluk E (2012) Numerical modeling of non-deformable support in swelling and squeezing rock. Int J Rock Mech Min Sci 52:61–70

Alm O (1982) The effect of water on the mechanical properties and microstructures of granitic rock at high pressure and high temperature. Proceedings of the 23rd Symposium on Rock Mechanics, University of California, Berkeley, California, August 25-27. New York: Society of Mining Engineers of the American Institute of Mining, Metallurgical and Petroleum Engineers, pp. 261–269

Anagnostou G (1993) A model for swelling rock in tunnelling. Rock Mech Rock Eng 26(4):307–331

Aydan O, Dalgic S (1998) Prediction of deformation behavior of 3 lanes Bolu tunnels through squeezing rocks of North Anotolian Fault Zone (NAFZ). Proceedings of the Regional Symposium on Sedimentary Rock Engineering, Taipei, pp. 228–233.

Aydan O, Akagi T, Kawamoto T (1993) The squeezing potential of rocks around tunnels: theory and prediction. Rock Mech Rock Eng 26(2): 137–163

Aydan O, Akagi T, Ito T, Ito J, Sato J (1995) Prediction of deformation behaviour of a tunnel in squeezing rock with time dependent characteristics. In: Proceedings of numerical models in geomechanics NUMOG V, pp. 463–469

Aydan O, Akagi T, Kawamoto T (1996) The squeezing potential of rock around tunnels: theory and prediction with examples taken from Japan. Rock Mech Rock Eng 29:125–143

Barla G (1995) Squeezing rocks in tunnels. ISRM News J II(3–4):44–49

Barla G, Bonini M, Semeraro M (2011) Analysis of the behaviour of a yield-control support system in squeezing rock. Tunn Undergr Space Technol 26:146–154

Bieniawski ZT (1974) Geomechanics classification of rock masses and its application in tunneling. Proceedings of the Third International Congress on Rock Mechanics, Vol. 11A. Denver: International Society of Rock Mechanics, pp. 27–32

Bieniawski ZT (1989) Engineering rock mass classifications. Wiley, New York, p 251

Bizjak KF, Petkovsek B (2004) Displacement analysis of tunnel support in soft rock around a shallow highway tunnel at Golovec. Eng Geol 75:89–106

Brox D, Hagedorn H (1999) Extreme deformation and damage during the construction of large tunnels. Tunn Undergr Space Technol 14(1): 23–28

Cantieni L, Anagnostou G (2009) The interaction between yielding supports and squeezing ground. Tunn Undergr Space Technol 24:309–322

Dalgic S (2002) Tunneling in squeezing rock, the Bolu tunnel, Anatolian motorway, Turkey. Eng Geol 67:73–96

Duda M, Renner J (2012) The weakening effect of water on the brittle failure strength of sandstone. Geophys J Int 192(3):1091–1108

Duncan FME (1993) Numerical modeling of yield zones in weak rocks.In comprehensive rock engineering. Rock Mech Min Sci 36(6):777–809

Erguler ZA, Ulusay R (2009) Water-induced variations in mechanical properties of clay-bearing rocks. Int J Rock Mech Min Sci 46(2): 355–370

GB/T 50266-2013 (2013) Standard for test methods of engineering rock mass, Beijing: China Planning Press

GB/T 50218-2014 (2014) Standard for Engineering Classification of Rock Mass. Beijing: China Planning Press

Gioda G, Cividini A (1996) Numerical methods for the analysis of tunnel performance in squeezing rocks. Rock Mech Rock Eng 29(4):171–193

Hadizadeh J, Law RD (1991) Water-weakening of sandstone and quartzite deformed atvarious stress and strain rates. Int J Rock Mech Min Sci Geomech Abstr 28(5):431–439

Haimson BC, Cornet FH (2003) ISRM suggested methods for rock stress estimation—part 3: hydraulic fracturing (HF) and/or hydraulic testing of pre-existing fractures (HTPF). Int J Rock Mech Min Sci 40(7–8):1011–1020

Hayashi K, Ito T (1993) In situ stress measurement by hydraulic fracturing at the Kamaishi mine. Int J Rock Mech Min Sci Geomech Abstr 30(7):951–957

Hisatake M, Ohno S, Katayama T, Ohmae Y (2012) Effects of the ring-cut method as a settlement deterrent in a soft ground tunnel. Tunn Undergr Space Technol 28:90–97

Hisatake M, Ohno S, Katayama T, Ohmae Y, Sano S (2009) Effects of the ring-cut excavation method on the restraint of displacements ahead of a tunnel face. Tunn Undergr Space Technol 24:547–554

Hsiao FY, Wang CL, Chern JC (2009) Numerical simulation of rock deformation for support design in tunnel intersection area. Tunn Undergr Space Technol 24:14–21

Hoek E (2001) Big tunnels in bad rock. J Geotech Geoenviron 127(9): 726–740

Hoek E, Guevara R (2009) Overcoming squeezing in the Yacambu-Quibor tunnel, Venezuela. Rock Mech Rock Eng 42:389–418

Hoek E, Marinos P (2000) Predicting tunnel squeezing problems in weak heterogeneous rock masses. Tunnels Tunnelling Int 32(11):45–51

Jiang Q, Jiang Y, Cui J, Feng X (2014) Application of computerized tomographic scanning to the study of water-induced weakening of mudstone. Bull Eng Geol Environ 73:1293–1301

Kalamaris GS, Bieniawski ZT (1995) A rock mass strength concept for coal incorporating the effect of time. Proceedings of the Eighth International Congress on Rock Mechanics. Vol. 1. Rotterdam: Balkema, pp. 295–302

Kavvadas M (2005) Monitoring ground deformation in tunnelling: current practice in transportation tunnels. Eng Geol 79(1–2):93–113

Khanlari G, Meybodi RG, Mokhtari E (2012) Engineering geological study of the second part of water supply Karaj to Tehran tunnel with emphasis on squeezing problems. Engineering Geology 145–146(3): 9–17

Kovfiri K, Staus J (1996) Basic considerations on tunnelling in squeezing ground. Rock Mech Rock Eng 29(4):203–210

Kuriyagawa M, Kobayashi H, Matsunaga I, Yamaguchi T, Hibiya K (1989) Application of hydraulic fracturing to three-dimensional in situ stress measurement. Int J Rock Mech Min Sci Geomech Abstr 26(6):587–593

Matsunaga I, Kuriyagawa M, Sasaki S (1989) In situ stress measurements by the hydraulic fracturing method at Imaichi pumped storage power plant, Tochigi, Japan. Int J Rock Mech Min Sci Geomech Abstr 26(3–4):203–209

Meng LB, Li TB, Jiang Y, Wang R, Li YR (2013) Characteristics and mechanisms of large deformation in the Zhegu mountain tunnel on the Sichuan-Tibet highway. Tunn Undergr Space Technol 37:157–164

Mezger F, Ramoni M, Anagnostou G (2017) Evaluation of higher capacity segmental lining systems when tunneling in squeezing rock. Tunn Undergr Space Technol 65:200–214

Nakano R (1979) Geotechnical properties of mudstone of neogene tertiary in Japan. Int Syrup Soil Mech Oaxaca 1:75–92

Sheorey PR (1997) Empirical Rock Failure Criteria. Balkema, Rotterdam

Singh M, Singh B, Choudhari J (2007) Critical strain and squeezing of rock mass in tunnels. Tunn Undergr Space Technol 22:343–350

Steiner W (1996) Tunnelling in squeezing rocks: case histories. Rock Mech Rock Eng 29(4):211–246

Sterpi D, Gioda G (2009) Visco-plastic behaviour around advancing tunnels in squeezing rock. Rock Mech Rock Eng 42:319–339

Tan JK, Kang WF (1980) Locked in stresses, creep and dilatancy of rocks, and constitutive equations. Rock Mech 13:5–22

Teng HW, Ren S, Jiang DY, Yang CH (2010) Experimental study of mechanical properties of water-saturated weaken shale in Gonghe tunnel. Chin J Rock Mech Eng 29(S1):2657–2662

Trueman R (1998) An evaluation of strata support techniques in dual life gateroads. Ph.D Thesis. University of Wales, Cardiff

Van Eeckhout EM (1976) The mechanisms of strength reduction due to moisture in coal mine shales. Int J Rock Mech Min Sci Geomech Abstr 13(2):A22

Walton G, Delaloye D, Diederichs MS (2014) Development of an elliptical fitting algorithm to improve change detection capabilities with applications for deformation monitoring in circular tunnels and shafts. Tunn Undergr Space Technol 43:336–349

Wang MY, Zhang N, Li J, Ma LJ, Fan PX (2015) Computational method of large deformation and its application in deep mining tunnel. Tunn Undergr Space Technol 50:47–53

Wood AM (1972) Tunnels for road and motorways. Q J Eng Geol 5:119–120

Yang TH, Xu T, Liu HY (2014) Rheological characteristics of weak rock mass and effects on the long-term stability of slopes. Rock Mech Rock Eng 47:2253–2263

Yassaghia A, Salari-Rad H (2005) Squeezing rock conditions at an igneous contact zone in the Taloun tunnels, Tehran-Shomal freeway, Iran: a case study. Int J Rock Mech Min Sci 42:95–108

Yilmaz I (2010) Influence of water content on the strength and deformability of gypsum. Int J Rock Mech Min Sci 47(2):342–347

Zhu JB, Wang B, Yang HP, Hu JM (2007) Experimental study on rheological mechanical properties of shale under unloading condition. Chin J Rock Mech Eng 26(Supp.2):4552–4556

Zhu XJ (1996) Characteristics of soft rocks interacting with water. Scientific Technol Min 4(3):46–50